

Applicability of compressible LES to reproduction of sound vibration of an air-reed instrument

Masataka Miyamoto (1), Yasunori Ito (1) Kin'ya Takahashi (1)
Toshiya Takami (2) Taizo Kobayashi (2) Akira Nishida (2) Mutsumi Aoyagi (2)

(1) The Physics Laboratories, Kyushu Institute of Technology, Kawazu 680-4, Iizuka 820-8502, Japan

(2) Research Institute for Information Technology, Kyushu University,
6-10-1 Hakozaki, Higashi-ku, Fukuoka 812-8581, Japan

PACS: 43.75.Qr,43.75.Np,43.75.Ef,43.75.-z,43.28.Ra

ABSTRACT

Sounding of a two dimensional(2D) small air reed instrument with an open end was numerically studied with compressible Large-Eddy Simulation (LES). Open end reflection of a 2D pipe reproduced numerically shows good agreement with that given by the theoretical formula developed by ourselves. Vibrations of the air-reed instrument driven by an air jet were well reproduced. The spatial distribution of aerodynamic sound source calculated with Lighthill's formula almost overlaps with that of vorticity near the mouth opening. The pressure detected at a point in the pipe vibrates at the fundamental or 2nd harmonic resonance frequency of the pipe depending on the jet velocity. So it strongly correlates with the jet oscillation. The relation of the sound frequency with the jet velocity was discussed comparing with the prediction given by the semi-empirical theory developed by Cremer & Ising, Coltman and other authors.

INTRODUCTION

Elucidation of acoustical mechanism of air-reed instruments is a long standing problem in the field of musical acoustics(1, 2). The major difficulty of numerical calculation of air-reed instrument is in strong and complex interactions between sound field and air flow dynamics(1, 2, 3), which is hardly reproduced by hybrid methods normally used for analysis of aero-acoustic noises(4). We need a direct method which allows to simulate dynamics of the jet flow and sound field in a resonator simultaneously.

With recent improvement in computer performance, direct simulations based on fluid dynamics becomes applicable for study of the sounding mechanism of air reed instruments. Yagawa and his coworkers used a node-by-node finite element method (NBN-FEM) for the direct calculation of the edge tone(5) Their result shows a good agreement with the experimental data(6). However, this method was not able to reproduce pipe resonance, because the open end reflection was not reproduced by their method(7). The lattice Boltzmann method (LBM) has been used for a direct simulation of air-reed instruments in MIT(8). It has succeeded in simulating the vibration of the jet(8, 9). But the result is still not realistic, because the method used requires a nonphysically high viscosity to stabilize oscillations.

The aim of our study is to reproduce sound vibration of air-reed instruments and to analyze the interaction of the jet flow with the sound field(10). To do this, we choose compressible Large-eddy Simulation (LES) solver to reproduce the sound field and flow dynamics of the instrument by directly solving the Navier Stokes equation, because LES is very stable for a long term calculation, though it somewhat sacrifices accuracy(4).

Taking a 2D small air-reed instrument with an open end, we have investigated how LES reproduces sound vibrations in the resonator as well as the jet oscillation as a sound source. Be-

fore that we will check the numerical reproducibility of the open end reflection of a 2D pipe with compressible LES, compared with the reflectance obtained by the theoretical formula for 2D flanged pipes developed ourselves. Numerical results are in good agreement with the theoretical prediction.

Next, the sound vibrations in the resonator as well as the jet oscillation are successfully reproduced for the 2D small air-reed instrument. Spatial distributions of air density, flow velocity, vorticity and Lighthill's sound sources are calculated. Further, the relation of the sound frequency with the jet velocity qualitatively was studied. It agrees with theoretical prediction by the semi-empirical theory developed by Cremer & Ising, Coltman and other authors based on experimental results (11, 12, 13, 14, 15, 16, 17, 18, 19, 20).

LIGHTHILL'S THEORY

The sound generated by turbulence is usually called aerodynamics sound, which is a very small byproduct of the motion of unsteady flows of high Reynolds number. The source of aerodynamics sound was clarified and given the exact form by Lighthill(21). Lighthill transformed exactly the set of fundamental equations, Navier-Stokes and continuity equations, to an inhomogeneous wave equation whose inhomogeneous term plays the role of the source:

$$\left(\frac{\partial^2}{\partial t^2} - c_0^2 \nabla^2\right)(\rho - \rho_0) = \frac{\partial^2 T_{ij}}{\partial x_i \partial x_j}, \quad (1)$$

where the tensor T_{ij} is called Lighthill's tensor and is defined by

$$T_{ij} = \rho v_i v_j + ((p - p_0) - c_0^2(\rho - \rho_0))\delta_{ij} + \sigma_{ij}. \quad (2)$$

Here, c_0 denotes the speed of sound in a stationary acoustic medium, p the air pressure with the average p_0 , ρ the air density with the average ρ_0 , and σ_{ij} the viscous stress tensor. It is considered that the sound wave is generated by the quadrupole

source distribution in turbulence given by the inhomogeneous term in RHS of eq.(1) and propagates like that in the stationary acoustic medium. This interpretation is called Lighthill's acoustic analogy.

Since the dissipation by σ_{ij} can be ignored for a high Reynolds number and adiabaticity is well held as

$$(p - p_0) - c_0^2(\rho - \rho_0) = 0, \quad (3)$$

then the first term of eq.(2), $\rho v_i v_j$, becomes the major term of the source. Further, particle velocities of the sound are usually sufficiently small compared with those of the real flow and so the source term is well approximated by that obtained from incompressible fluid with $\rho = \rho_0$ and $\text{div } \mathbf{v} = 0$. Then, the sound source is given by

$$\begin{aligned} \frac{\partial^2 T_{ij}}{\partial x_i \partial x_j} &\sim \rho_0 \frac{\partial^2 v_i v_j}{\partial x_i \partial x_j} \\ &= s_{ij}^2 - w_{ij}^2 \\ &= \rho_0 \text{div}(\boldsymbol{\omega} \times \mathbf{v}) + \rho_0 \nabla^2 \left(\frac{1}{2} v^2 \right), \end{aligned} \quad (4)$$

where s_{ij} and w_{ij} are respectively given by

$$s_{ij} = \frac{1}{2} \left(\frac{\partial v_j}{\partial x_i} + \frac{\partial v_i}{\partial x_j} \right) \quad (5)$$

$$w_{ij} = \frac{1}{2} \left(\frac{\partial v_j}{\partial x_i} - \frac{\partial v_i}{\partial x_j} \right). \quad (6)$$

For two dimensional(2D) fluid, it is further reduced into

$$\frac{\partial^2 T_{ij}}{\partial x_i \partial x_j} \sim -2\rho_0 \left(\frac{\partial v_1}{\partial x_1} \frac{\partial v_2}{\partial x_2} - \frac{\partial v_2}{\partial x_1} \frac{\partial v_1}{\partial x_2} \right). \quad (7)$$

This formula will be used for calculation of Lighthill's sound sources later.

EDGE TONE

As shown in Fig.1, edge tone is an aerodynamics sound generated by the unsteady but mostly periodical oscillation of jet emanated from the flue and collided with the edge, which is consider as the sound source of air-reed instruments(1, 2, 3). Production of edge tone has been a long standing problem in the fields of aero-acoustics and musical acoustics and details of its mechanics are not completely understood yet. However, its features have been well captured by semi-empirical equations introduced based on experimental results. To the authors' knowledge, the first pioneer work was done by Brown, who introduced the following empirical formula(6):

$$f = 0.466j(100V - 40)(1/(100l) - 0.07), \quad (8)$$

where V denotes the speed of jet and l is the distance between the flue and the edge. The number j is taken as $j = 1.0, 2.3, 3.8, 5.4$. For $j = 1$, it gives the fundamental frequency and others denote overtones. With increase of V , the fundamental oscillation is excited and its frequency increases in proportion to V . But it jumps to one of overtones, if V exceeds a threshold value, and it jumps successively from one to other with increase of V . The transitions are hysteretic and so the the threshold values of V of the downward process are usually different from those of the upward.

Note that the edge tone in the 2D and 3D geometries are successfully reproduced by several schemes including the compressible LES used in our study(5, 22).

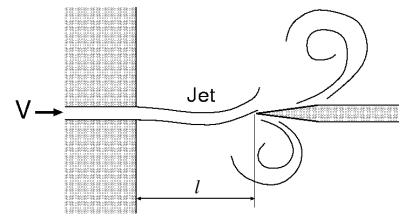


Figure 1: Edge tone

MODEL AND NUMERICAL SCHEME

A 2D model of air reed instruments, which we will study in this paper, is shown in Fig.2(a). Parameters which determine the dimensions of the model are indicated in the figure. The angle of the edge of 25° is determined referring to real air-reed instruments. In the numerical analysis, we use compressible LES(Large Eddy Simulation)(4) to solve a compressible fluid motion inside the air reed instrument as well as in the near field of it. In the LES method, the number of grid points is markedly saved with other analytical schemes. A fluid element such as a vortex bigger than the representative size of cells is analyzed directly. On the other hand, the feedback of vortexes smaller than the cell size to the macro-scale dynamics is approximates by using the statistical averaging procedure that is called SGS (sub-grid scale) model. Therefore, it is considered that LES does not reproduce the fluid dynamics with a high degree of accuracy in a boundary layer like a neighborhood of the edge in comparison with the other methods. However, it is suitable for long term simulations, because it is very stable. In our calculation, the time evolution up to 0.1s is considered. Taking into consideration the highness of the phase speed of sound waves, time step is taken at $\Delta t = 1.0 \times 10^{-7}$ s.

The numeric scheme used for the analysis is the compression LES solver "Coodles" in OpenFOAM ver1.5(23). The numerical mesh used for calculation is shown in Fig.2(b), and its parameters are shown in Table 1. The observation points are points **A** and **B** in Fig.2(a). Point **A** is located at the point on the center axis of the pipe 10.0mm left from the open end. At this point, the acoustic pressure (pressure displacement from the atmospheric pressure) is observed. Point **B** is 3.0mm right from the exit of the flue on its center axis. At this point, the vorticity that the jet produces is measured. According to the vortex sound theory(24, 25) that Powell and Howe developed following Lighthill's acoustic analogy(21), vortexes are the main source of the aerodynamic sound. This is the reason why the vorticity is measured.

Table 1: Parameters of mesh

points	cells	faces
193,212	95,662	383,592

OPEN-END REFLECTION

Before showing numerical results of the air-reed instrument introduced above, we see how open-end reflection is numerically reproduced by LES, because the reproducibility of the open end reflection is one of the bench mark tests how a compressible fluid solver effectively reproduces properties of acoustic waves. Indeed, it was reported that a sort of finite elementary methods, a compressible CFD scheme with node-by-node finite elements, is not available for the reproduction of open-end reflection(7), while a certain lattice Boltzmann method well reproduces the open end reflection of a axially symmet-

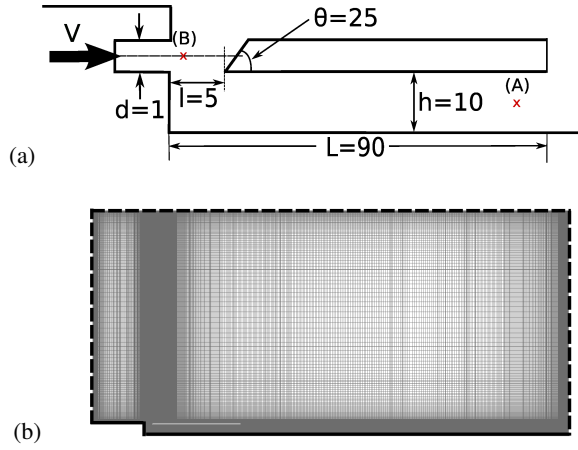


Figure 2: Model and mesh. (a) Dimensions of 2D model (Unit of length :mm; Unit of angle:degree). (b) Numerical mesh.

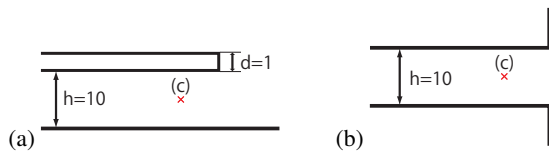


Figure 3: Two models for calculation of open-end reflection. (a) Model 1. (b) Model 2.

ric pipe(26) and it was also reported that sounding of air-reed instruments is partially reproduced by some other type of the lattice Boltzmann method(9).

To check the numerical reproducibility of the open end reflection of a 2D pipe with LES, we need the theory of the radiation impedance of 2D open pipes as a reference. The radiation impedance of a 2D flanged pipe, i.e., an open pipe set in an infinite plane baffle, is obtained in a similar way of derivation to that of a 3D flanged pipe, for the case of 3D pipes see Ref.(27). First, a 2D cylindrical wave caused by a point source with a strength Q is given by

$$p(r) = \rho_0 c \frac{Qk}{2} H_0^{(2)}(kr) e^{i\omega t}, \quad (9)$$

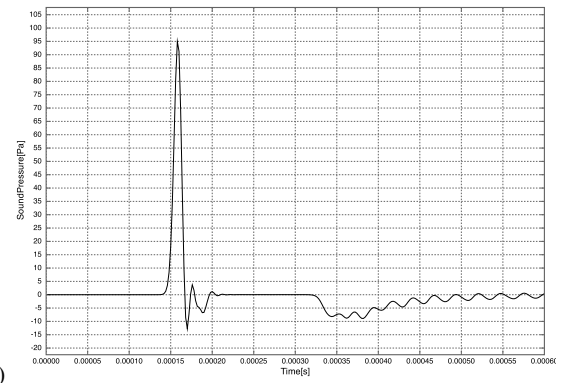
where $H_0^{(2)}$ is the 0-th order Hankel function of the second kind. Making use of this solution, the radiation impedance of a 2D flanged pipe with a height $h = 2a$ is obtained in a similar way for the case of a 3D flanged pipe:

$$\begin{aligned} Z_R(\omega) &= Z_0 \frac{k}{a} \int_0^a dr' \int_0^{2r'} dr H_0^{(2)}(kr) \\ &= Z_0 \frac{\pi k}{a} \int_0^a dr' r' \\ &\quad \times \left(\mathbf{H}_0(2kr') H_1^{(2)}(2kr') + \mathbf{H}_{-1}(2kr') H_0^{(2)}(2kr') \right), \end{aligned} \quad (10)$$

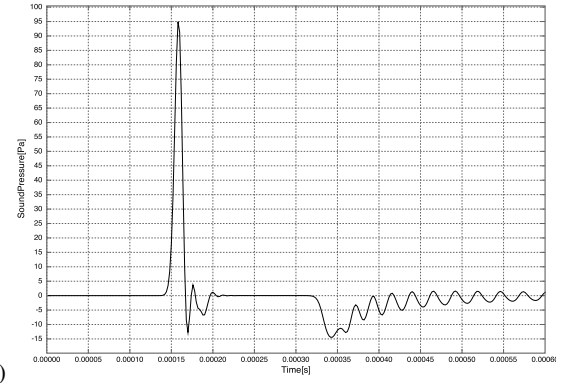
where $\omega = ck$, the characteristic impedance of the pipe Z_0 is given by $Z_0 = \rho_0 c / (2a)$ and \mathbf{H}_n denotes the Struve function. In the small and large limits of ω , Z_R is respectively reduced into

$$\lim_{\omega \rightarrow 0} Z_R(\omega) \sim -\frac{i}{2\pi} Z_0 k a \left(\log(ka) - \frac{1}{2} \right) \rightarrow 0, \quad (11)$$

$$\lim_{\omega \rightarrow \infty} Z_R(\omega) \rightarrow Z_0 + O(1/\omega). \quad (12)$$



(a)



(b)

Figure 4: Time evolution of an injected pulse observed at the fixed point (C) in Fig.3(a) and (b) (time step: $\Delta t = 1.0 \times 10^{-7}$ s). (a) Change of acoustic pressure for Model 1. (b) Change of acoustic pressure for Model 2.

From Z_R obtained with numerical integration, the reflectance R is calculated through the following formula,

$$R(\omega) = \left| \frac{Z_R - Z_0}{Z_R + Z_0} \right|^2. \quad (13)$$

The end correction ΔL is also obtained with

$$\Delta L(\omega) = \frac{1}{2k} \arg \left(-\sqrt{R} \frac{Z_R + Z_0}{Z_R - Z_0} \right) \quad (14)$$

$$\sim \frac{2a}{\pi} \left(\frac{1}{2} - \log ak \right), \quad (\omega \ll 1), \quad (15)$$

where the evaluation in the most RHS term is given by making use of eq.(11).

We will show numerical results for two pipe models with different shapes of opening(see Fig.3). The first model in Fig.3(a) (Model 1) has the same opening as the air-reed instrument in Fig.2. The second model(Model 2) in Fig.3 (b) is of a flanged opening. A Gaussian-shape pulse is injected from the left hand side in the pipe and the time evolution of acoustic pressure is observed at the point (c) between the input point of the pulse and the opening(see Fig.3 (a) and (b)). For both models, as shown in Fig.4, the positive incident pulse is reflected at the open end and comes back as a negative pulse. However, the reflective pulses are fairly deformed with smaller amplitudes and are accompanied by a long oscillating tail. The frequency of the oscillation is of about 39000Hz, nearly equal to twice the cutoff frequency f_c defined as $f_c = c/2a \sim 17394$ Hz. It means that the second mode instead of the first mode is excited on the cross section of the pipe. The amplitude of the reflective

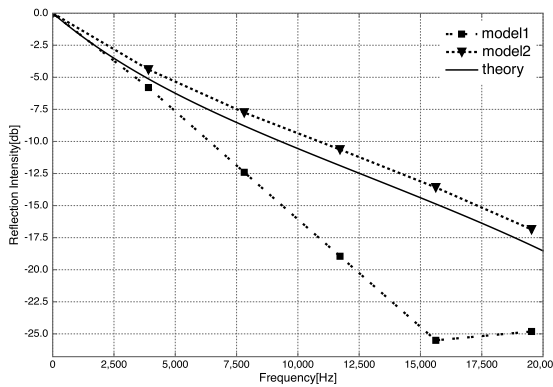


Figure 5: Reflected intensities obtained numerically for Model 1 and 2 compared with the theoretical calculation given by eq.(13)

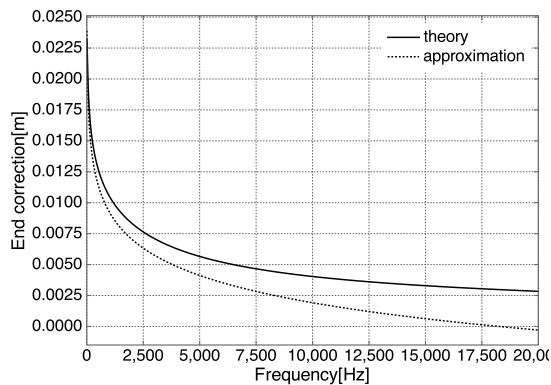


Figure 6: End corrections obtained by eqs.(14) and (15).

pulse for Model 2 is larger than that for Model 1. In any case, it seems that the open end reflection is reproduced by the numerical calculation with LES.

Fig.5 shows reflected intensities for the two models as a function of frequency, which are obtained with taking the ratio of the power spectrum of the output pulse to that of the input. For comparison, the reflectance R obtained theoretically with eq.(13) is also drawn in this graph. All the reflected intensities decrease exponentially with the frequency f in the range ($0 \leq f \leq f_c$). However, the reflection intensity for Model 1 is fairly smaller than that for Model 2, though the reflected intensity for Model 2 decreases with almost the same rate as that given by the theoretical formula for flanged pipes. Then the compressible LES well reproduces the open end reflection. However, Model 1 has weak resonances compared with Model 2. This is because Model 1 has no sharp edge nor flange at the bottom of the opening, which makes the reflectivity reduced. The reason why we take Model 1 with a smaller reflectance rather than Model 2 with a stronger one is to reduce a numerical elapse time with decreasing the number of the grid points. Fig.6 shows end corrections obtained by eqs.(14) and (15). The approximation given by eq.(15) well follows the exact formula of eq.(14) in a low frequency range. The end corrections are estimated as $\Delta L \sim 9.0\text{mm}$ and $\Delta L \sim 6.9\text{mm}$ at the first and second resonance of the pipe, $f \sim 1611\text{Hz}$ and $f \sim 3221\text{Hz}$, respectively.

NUMERICAL RESULTS

Stable oscillation

In this subsection, we shows results at $V = 26\text{m/s}$, at which the most stable oscillation of the fundamental state is observed. Fig.7 shows the spatial distributions of air density, flow velocity, vorticity and Lighthill's sound source observed at a certain time. Lighthill's sound source is calculated by using eq.(7). In the air density distribution in Fig.7(a), we see a stationary oscillation with a large amplitude inside the pipe, while the air density takes smaller values in the amplitude in the outside. As shown in Fig.7 (b), the jet is oscillating regularly and there exist large eddies rolled up near the mouth over and under the edge, which are created by the collision of the jet with the edge. The distribution of Lighthill's sound source in Fig.7 (c) almost overlaps with that of the vorticity in Fig.7 (d). This result agrees with Powell-Howe vortex sound theory(24, 25), which claims that the major part of the sound is emitted by moving vortexes.

Fig.8 shows time evolution of the acoustic pressure and its power spectrum at the observation point **A**. The amplitude of the wave fluctuates in some beat pattern, but the pitch is kept at the almost same value 1514Hz after a short starting transient.

Fig.9 shows time evolution of the vorticity and its power spectrum at the observation point **B**. Vorticity oscillates with the amplitude more stable compared with the acoustic pressure. The power spectrum has the peak of the fundamental pitch at 1514Hz, which is the same as that of the acoustic pressure. It means that the jet motion is synchronized with the sound field of the fundamental resonance of the pipe.

Change of frequency with jet velocity

In Fig.10 we shows the change of frequency of the acoustic pressure at the point **A** with increase of V . The pipe resonance frequencies given by the acoustic theory and the edge tone frequency given by Brown's edge tone equation in eq.(8) are also depicted in this figure.

The frequency curve of the fundamental changes linearly following Brown's edge tone equation in range of $V = 2 \sim 18\text{m/s}$. But, for $V \geq 20\text{m/s}$, the curve levels off approaching to the fundamental resonance frequency of the pipe, which means that the frequency rocking to the fundamental occurs. The first overtone observed for $V \geq 30\text{m/s}$ increases following the Brown's edge tone equation in the beginning and is leveled off converging on the second harmonic. From the observation of pressure waves, which are not shown here though, it seems that the transition from the fundamental to the second harmonics takes place beyond $V = 32\text{m/s}$. Indeed, the wave form is change from a fundamental wave to a second harmonic wave.

The characteristic of the frequency change with respect to V qualitatively agrees with the theoretical prediction by Cremer & Ising, Coltman and other authors. It supports the validity of our numerical analysis and it is safely said that the compressible LES reproduces sound vibrations of air-reed instruments.

DISCUSSION

In this paper, we reported reproducibility of open end reflection of 2D open pipes and of sound vibration of a 2D air-reed instrument with compressible LES. The reflection intensity of the 2D flanged pipe is well reproduced as a function of frequency by the compressible LES, which is confirmed with comparing with that given by the theoretical method developed by ourselves.

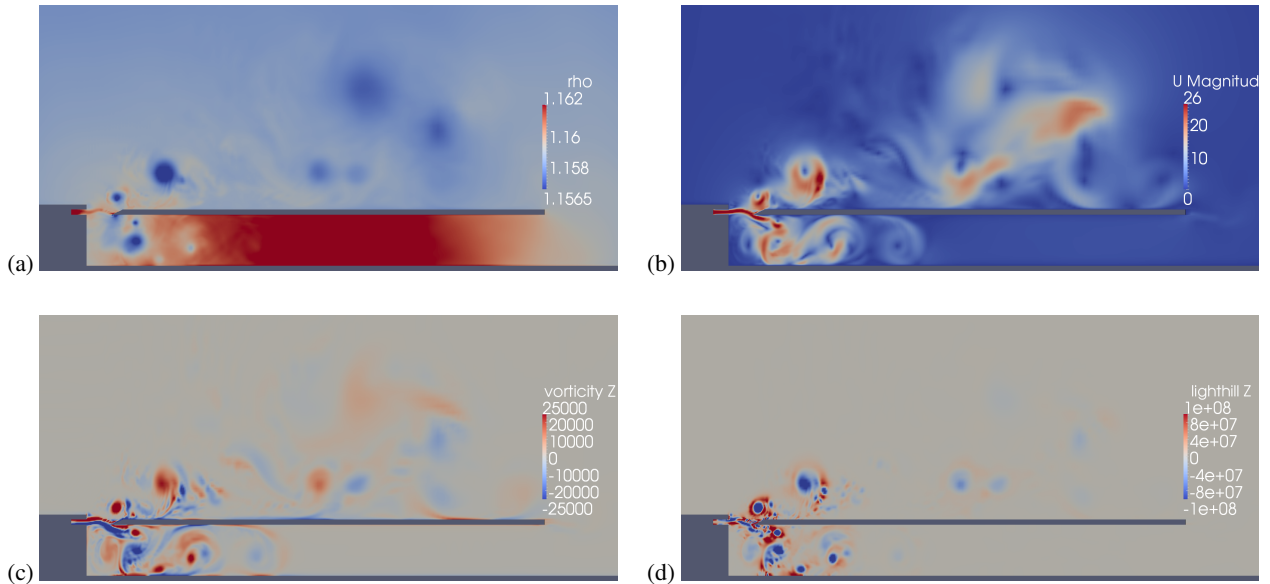


Figure 7: Spatial distributions of representative dynamical variables. (a) Air density. (b) Flow velocity. (c) Vorticity. (d) Lighthill's sound source.

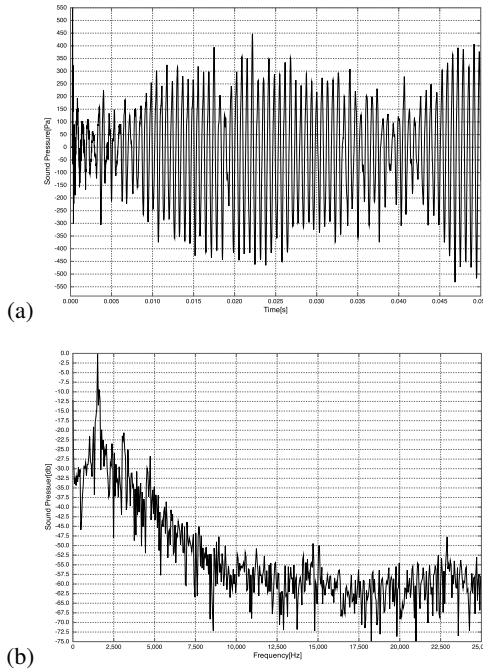


Figure 8: Acoustic pressure at point A. (a) Acoustic pressure oscillation. (b) Power spectrum.

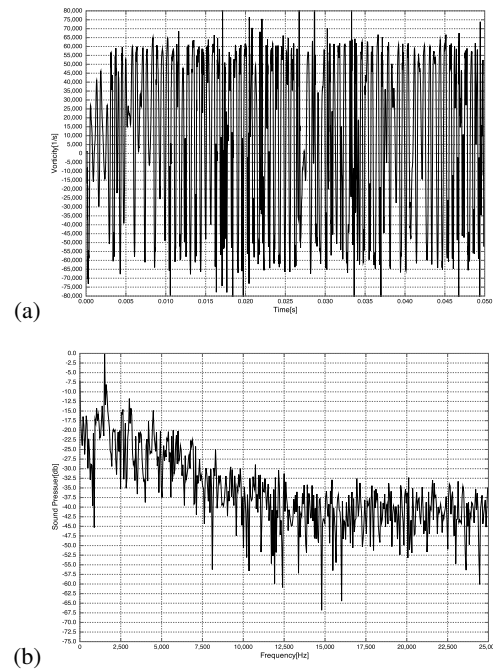


Figure 9: Vorticity at point B. (a) Vorticity oscillation. (b) Power spectrum.

Relying upon the successful reproduction of open end reflection, we have gone forward the calculation of the air-reed instrument with a open end. As a result, the jet oscillation and sound production of the air-reed instrument are well reproduced by using the compressible LES. Spatial distributions of characteristic dynamical variables, air density, flow velocity, vorticity and Lighthill's sound source, are calculated. The distributions of flow velocity and vorticity near the mouth opening are very similar to those observed experimentally (28, 29). Especially, change of the sound frequency with the jet velocity obtained numerically shows good agreement with the theoretical prediction as well as experimental results (11, 12, 13, 14, 15, 16, 17, 18, 19, 20). For more detail comparison of the nu-

merical result with the theoretical prediction, see Ref.(10), in which the air-reed instrument with a closed end instead of that with the open end was studied though.

Based on the results of this paper, we are able to proceed to comprehensively study the acoustic mechanism of the air-reed instrument. With help of the Lighthill theory(21) and/or Powell-Howe vortex sound theory(3, 24, 25), the place of sound sources in turbulence will be detected clearly and their behavior will be characterised in terms of aero-dynamics and nonlinear dynamics. We have already started the research for the problem of edge tone in this direction(22). We will have to answer the questions which mechanism, volume-flow mechanism or mo-

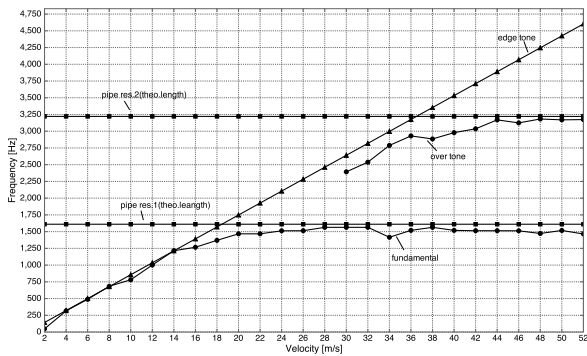


Figure 10: Changes of oscillation frequencies with jet velocity.

mentum drive mechanism (11, 12, 13, 14, 15, 20, 30, 31), dominates at a given jet velocity and what change occurs with change of the jet velocity. It is the most important to answer the problem what kind of interaction between the resonance of the pipe and the jet motion works to synchronize the fluid vibration with the sound oscillation. The synchronization mechanism should be different from that of the edge tone.

Concerning with 3D model calculation, we have already start the calculation of some model systems(22, 32). In Ref.(32), the 3D ocarina model was studied. The ocarina uses the Helmholtz resonance caused by an elastic property of air instead of the pipe resonance. Then, it is quite interesting to consider the problem how different acoustic mechanisms work for different types of resonator with comparing numerical data of the ocarina with that of a 3D model of the instrument with a resonance pipe.

ACKNOWLEDGEMENT

This work is supported by Grant-in-Aid for Exploratory Research No.20654035 from Japan Society for the Promotion of Science (JSPA).

REFERENCES

- [1] N. H. Fletcher and T. D. Rossing, *The Physics of Musical Instruments*, 2nd Edition (Springer-Verlag, New York 1998).
- [2] A. Hirschberg, "Aero-acoustics of Wind instruments." in "Mechanics of Musical Instruments," Eds. A.Hirschberg, J.Kergomard and G.Weinreich. (Springer-Verlag, Vienna and New York 1995), pp.291-369.
- [3] M. S. Howe, *Acoustics of Fluid-Structure Interactions*, (Cambridge Univ. Press, 1998).
- [4] C. Wagner, T. Hüttl, and P. Sagaut, eds. 'Large-Eddy Simulation for Acoustics,' (Cambridge Univ. Press, New York, 2007).
- [5] J. Tsuchida, T. Fujisawa, and G. Yagawa, "Direct numerical simulation of aerodynamic sounds by a compressible CFD scheme with node-by-node finite elements," *Computer Methods in Applied Mechanics and Engineering* **195** 1896-1910 (2006).
- [6] G. B. Brown, 'The vortex motion causing edge tones,' *Proc. Phys. Soc.*, London **XLIX** 493-507 (1937).
- [7] G.Yagawa *et al.*, unpublished.
- [8] P.A.Skordos, 'Modeling flue pipes: subsonic flow, lattice Boltzmann, and parallel Distributed computes', Ph. D. thesis, MIT (1995).
- [9] H. Kühnelt, "Simulating and sound generation in flutes and flue pipes with the Lattice-Boltzmann-Method," *Proc. of ISMA 2004*, Nara Japan, pp.251-254.

- [10] M. Miyamoto, Y. Ito, K. Takahashi, T. Takami, T. Kobayashi, A. Nishida, M.Aoyagi, 'Numerical study on sound vibration of an air-reed instrument with compressible LES', preprint, <http://arxiv.org/abs/1005.3413>.
- [11] L. Cremer and H. Ising, "Die selbsterregten Schwingungen von Orgelpfeifen," *Acustica* **19** 143-153 (1967).
- [12] J. W. Coltman, 'Sounding mechanism of the flute and organ pipe,' *J. Acoust. Soc. Am.* **44** 983-992 (1968).
- [13] J. W. Coltman, 'Acoustics of the flute,' *Physics Today* **21** 25-32 (1968).
- [14] J. W. Coltman, 'Jet driven mechanisms in edge tones and organ pipes,' *J. Acoust. Soc. Am.* **60** 725-733 (1976).
- [15] J. W. Coltman, 'Momentum transfer in jet excitation of flute-like instruments,' *J. Acoust. Soc. Am.* **69** 1164-1168 (1981).
- [16] N. H. Fletcher and S. Thwaites, "Wave propagation on an acoustically perturbed jet," *Acustica* **42** 323-334 (1979).
- [17] S. Thwaites and N. H. Fletcher, "Wave propagation on turbulent jets," *Acustica* **45** 175-179 (1980).
- [18] S. Thwaites and N. H. Fletcher, "Wave propagation on turbulent jets. II. Growth," *Acustica* **51** 44-49 (1982).
- [19] N. H. Fletcher and S. Thwaites, "The physics of organ pipes," *Scientific American* **248** 84-93 (1983).
- [20] N. H. Fletcher, "Jet-drive mechanism in organ pipes," *J. Acoust. Soc. Am.* **60** 481-483 (1976).
- [21] M. J. Lighthill, 'On sound generated aerodynamically. Part I: General theory,' *Proc. Roy. Soc. London* **A211** 564-587 (1952).
- [22] K. Takahashi, M. Miyamoto, Y. Ito, T. Takami, T. Kobayashi, A. Nishida, M.Aoyagi, 'Numerical analysis on 2D and 3D edge tones in terms of aerodynamic sound theory' to appear in *Proc. of ICA2010*.
- [23] <http://www.openfoam.com/>
- [24] A. Powell, 'Theory of vortex sound,' *J. Acoust. Soc. Am.* **36** 177-195 (1964).
- [25] M. S. Howe, 'Contributions to the theory of aerodynamic sound with application to excess jet noise and the theory of the flute,' *J. Fluid Mech.* **71** 625-673 (1975).
- [26] A. R. da Silva and G. P. Scavone, 'Lattice Boltzmann simulations of the acoustic radiation from waveguides', *J. Phys. A* **40** (2007) pp.397-408.
- [27] L.E. Kinsler, A.R.Frey, A.B. Coppens and J.V. Sanders, "Fundamentals of Acoustics" 4th Ed. (John Wiley & Sons, Inc. 2000).
- [28] B. Fabre, A. Hirschberg, A. P. J. Wijnands, "Vortex shedding in steady oscillation of a flue organ pipe," *Acta acustica, Acustica* **82** 863-877 (1996).
- [29] A. Bamberger, "Vortex sound of the flue," *Proceedings of ISMA2007*, Barcelona Spain, (CD-ROM ISBN:978-84-934142-1-4), 1-S1-5.
- [30] S. A. Elder, "On the mechanism of sound production on organ pipes," *J. Acoust. Soc. Am.* **54** 1554-1564 (1973).
- [31] S. Yoshikawa and J. Saneyoshi, "Feedback excitation mechanism in organ pipes," *J. Acoust. Soc. Jpn. (E)* **1** 175-191 (1980).
- [32] T. Kobayashi, T. Takami, M. Miyamoto, K. Takahashi, A. Nishida, and M.Aoyagi, '3D Calculation with Compressible LES for Sound Vibration of Ocarina,' *Open Source CFD International Conference 2009*, November 12-13th, Barcelona, Spain (CD-ROM).